GEODESY AND CARTOGRAPHY
Vol. 67, No. 2, 2018, pp. 207–238

© Polish Academy of Sciences
DOI: https://doi.org/10.24425/gac.2018.125472

Original research paper

Accuracy of Precise Point Positioning (PPP) with the use of different International GNSS Service (IGS) products and stochastic modelling

Damian Kiliszek[1]*, Marcin Szołucha[2], Krzysztof Kroszczyński[3]

[1,2,3]Military University of Technology, Faculty of Civil Engineering and Geodesy
2 Gen. W. Urbanowicza St. 00-908 Warsaw, Poland

[1]e-mail: damian.kiliszek@wat.edu.pl, ORCID: http://orcid.org/0000-0002-5466-997
[2]e-mail: marcin.szolucha@wat.edu.pl, ORCID: http://orcid.org/0000-0002-7349-0990
[3]e-mail: krzysztof.kroszczynski@wat.edu.pl, ORCID: http://orcid.org/0000-0003-1197-9915

*Corresponding author: Damian Kiliszek

Received: 2 October 2018 / Accepted: 10 November 2018

Abstract: This paper provides analyses of the accuracy and convergence time of the PPP method using GPS systems and different IGS products. The official IGS products: Final, Rapid and Ultra Rapid as well as MGEX products calculated by the CODE analysis centres were used. In addition, calculations with weighting function of the observations were carried out, depending on the elevation angle. The best results were obtained for CODE products, with a 5-minute interval precision ephemeris and precise corrections to satellite clocks with a 30-second interval. For these calculations the accuracy of position determination was at the level of 3 cm with a convergence time of 44 min. Final and Rapid products, which were orbit with a 15-minute interval and clock with a 5 minute interval, gave very similar results. The same level of accuracy was obtained for calculations with CODE products, for which both precise ephemeris and precise corrections to satellite clocks with the interval of 5 minutes. For these calculations, the accuracy was 4 cm with the convergence time of 70 min. The worst accuracy was obtained for calculations with Ultra-rapid products, with an interval of 15 minutes. For these calculations, the accuracy was 10 cm with a convergence time of 120 min. The use of the weighting function improved the accuracy of position determination in each case, except for calculations with Ultra-rapid products. The use of this function slightly increased the convergence time, in addition to the CODE calculation, which was reduced to 9 min.

Keywords: accuracy, PPP, convergence time, IGS products, stochastic modelling

1. Introduction

Surveying based on data from Global Navigation Satellite System (GNSS) systems in most cases is associated with relative methods. Using phase observations from at least two points, precise baseline ΔX, ΔY, ΔZ could be determinated and depending on the

accuracy requirements, this calculations could be process in real time – Real Time Kinematic (RTK) / RTK Network (RTN) (Paziewski and Wielgosz, 2017; Grejner-Brzezinska et al., 2005; Prochniewicz et al., 2016) or in postprocessing – static method (Hofmann-Wellenhof et al., 2008).

In the last 20 years a significant development of another method can be noticed: Precise Point Positionig (PPP), which is characterized by a similar level of accuracy and where calculations are based on data from only one receiver (Kouba, 2017). This is possible due to significant technical development, such as the improvement of computational algorithms or increase of the quality of products within the GNSS (Kouba, 2015; Kouba, 2017). However, the PPP method requires external data like precise satellite location information and the characteristics of their on-board clocks (GNSS products). Basically these products coming from data of global reference station networks, e.g. the International GNSS Service (IGS) network (Multi-GNSS Experiment (MGEX); Real Time Service (RTS)). The lack of direct connection between the determined receiver position and reference networks means that this method is not dependent on the length of the vector so it does not transfer errors. Additionally any connection with the reference station and the data center is require – what is particularly important in real time measurements, where interruptions in data transmission can happened. From the other hands a big limitation of the PPP method is the time of convergence. This factor significantly limits the possibilities of determination of the receiver position. This time is associated with a strong correlation between the receiver clock, height receiver, tropospheric delay and ambiguities which is strongly associated with hardware delays both satellite and the receiver (Witchayangkoon, 2002; Kalita, 2017). In addition, the accuracy of PPP depends on the number of satellites observed and their distribution-geometry (Li et al., 2015; Cai et al., 2015; Kaźmierski et al., 2018). The accuracy of PPP positioning also depends on the quality of GNSS products: the orbits and clock corrections, especially the latter have a significant impact (Guo et al., 2010).

Generally the PPP method was first proposed by Zumberge in 1997, where its primary goal was only to increase the accuracy of the position of the receiver performing the measurement in SPP mode. At present the PPP is applied in: precise determination of the coordinates of the receiver, e.g. geodesy, navigation (Krzan and Stępniak, 2017; Kostelecký et al., 2015); weather forecasting, e.g. data assimilation (Hadaś et al., 2013; Dousa and Vaclavovic, 2014); estimation of orbits – mainly low elevation and real time orbits (Li et al., 2015); determination of the tropospheric delay, e.g. water vapor content in the atmosphere (Li et al 2014b; Ahmed et al., 2016; Gołaszewski et al., 2017; Bałdysz et al., 2018); radio-occultation (Shi and Gao, 2009); estimation of satellite clocks correction (Lou et al., 2014); system monitoring in earthquakes areas (Li et al., 2014a; Geng et al., 2013); tsunami warning systems (Hoechner, 2013); monitoring of time scales generated (Cerretto et al., 2012) or unmanned aerial vehicle photogrammetry (Tsai et al., 2013). Presently the PPP method can achieve accuracy of around mm-cm for static measurements and around cm-dm for kinematic survey in real-time mode. This causes the increase of applicability of this method not only for static purpose but also in real-time measurements.

The basic PPP model uses un-differenced code and phase observations from two frequencies which are transformed into a linear ionosphere-free combination, eliminating the first-order ionospheric delay (Kouba and Heroux, 2001). The disadvantage of this combination is non-integer character of ambiguities. The other PPP models developed for reduction of convergence time and improve the accuracy of the obtained coordinates are:

- one of the most effective PPP models use the differentiation between the satellites – BSSD (Between-Satellite Single-Difference). It eliminates errors related to the receiving system of the receiver, which reducing convergence time and increasing the accuracy of the position, also facilitates the integration of multi-GNSS (Abd Rabbou and El-Rabbany, 2015; Elsobeiey and El-Rabbany 2013 and 2014; Afifi and El-Rabbany 2016; Nykiel and Figurski, 2016);
- another interesting model is the model proposed by Collins et al. (2010), which separates the receiver clock correction for phase and code measurements;
- the PPP-RTK model uses un-differenced raw observations, in which integer ambiguities are determined with the use of network solutions (Li et al., 2014a; Khodabandeh and Teunissen, 2015; Teunissen et al., 2010; Ge et al., 2008);
- models that use higher order ionosphere corrections can also increase the accuracy (Banvile et al., 2017, Liu et al., 2016);
- another solution are models that integrate several GNSS systems – multi-GNSS. Using multi-GNSS receivers causes that more satellites could be observed what ignificantly improves the geometry of the solution. Thanks to this all measurements are corrected, i.e. kinematic and static, both differential and non-differential in real time or postprocessing (Yu and Gao, 2017; Abd Rabbou and El-Rabbany , 2015; Rabbou Abd and El-Rabbany A, 2016; Cai et al., 2015; Li et al., 2015; Tegedor et al., 2014; Ge et al., 2017, Liu et al., 2017; Wang et al., 2018).

For differential measurements, satellite orbit and satellite clocks errors are eliminated by using double difference equations (Hofmann-Wellenhof et al., 2008). However, due to the lack of differentiation of measurements with reference station in PPP method the accuracy of GNSS products directly affects the final accuracy of the method (Lou et al., 2014). For this purpose, it is recommended to use products designated from the global network of the IGS reference stations (Kouba, 2015).

The accuracy of the PPP solution is closely related to the accuracy of data generated from observation of global networks. From the very beginning of the IGS service (1994), the quality of this products continuously increase, both in orbits and satellite clocks (Kouba, 2015). Initially the errors in the designation of products, both official – combined and each Center Analysis (AC) were at the level of several dozen cm (about 30 cm). However, from 1400 week GPS (5 November 2006), the accuracy of products maintains constant accuracy of 1–2 cm. In previously mentioned paper, it was shown how the accuracy of the PPP method with IGS products increased from the level of cm to the level of mm, for precise PPP calculations in postprocessing.

Initialy method of stochastic modeling of GNSS observations has an assumption that all measurements from each satellite are of the same accuracy, and observations weighting are made only according to the angle of the satellite elevation (Yu and Gao, 2017).

At the work Kaźmierski et al. (2018) it has been shown that by different stochastic modeling of observations can either improve or decrease the accuracy as well as reduce or increase the convergence time of the determined position. In mentioned work, however, this has been analyzed as intra- or inter-system weights using different GNSS systems. For each GNSS system, as well as for individual generation-blocks of satellites or the type of orbits, as in the BeiDou Navigation Satellite System (BDS), other errors have been accepted. In the work of Yu and Gao (2017), stochastic modeling was divided into two methods, in which the criterion of weighting the observations was adopted depending on the satellite elevation mask, divided into two weighting functions. The first $\sin\theta$ is for satellites with an elevation mask above 30° while the second one $\sin^2\theta$ is for satellites with an elevation mask below 30°. The authors of GNSS-Lab Tool (gLAB) software recommend performing observation weights through the adopted algorithm used by the Minimum Operational Performance Standard (MOPS), which is used to reduce the multipath effect (RTCA-MOPS, 2006). This function is exponential based on elevation-angle stochastic model, but the disadvantage of the proposed algorithm is that both code and phase measurements has the same weights, which is not sufficient for the basic PPP model as it uses both code and phase observations. This function was used in the work of Hans, 1997, but for double-difference measurements. However, the coefficients in this work had different values for code observations and for phase observations. The use of such function improves the accuracy of position determination and increase correctly determined of ambiguities. The same function as in the work of Hans, 1997, with the same values of coefficients, was used in the work of Gao et al., 2011 for PPP positioning. In this case the function being used resulted in decreasing of accuracy in relation of simple weighting i.e, the observation errors for each satellite are the same regardless of the elevation angle. In the aforementioned work (Gao et al., 2011), stochastic modeling was also carried out using carrier-to-noise-power density ratio (C / No), which also caused a deterioration in accuracy compared to a simple weighting, but a little less than exponential-function. Another way was to combine the two functions, which this time increased the accuracy of PPP positioning.

In presented research, the authors decided to check what accuracy is possible to be achieved of determination of the position, using the PPP method with only the GPS system, using various IGS products and both official – combined (Final, Rapid, Ultra rapid) as well as those calculated by one AC Center for Orbit Determination in Europe (CODE). The calculations were carried out using the gLAB software, using 4 stations of the EUREF Permanent GNSS Network (EPN) network, situated in Poland. Observations were carried out for one full day (arbitrary chosen November 25, 2017), divided into 3 hour measurement sessions. The obtained results were compared with the EPN reference coordinates. In addition, calculates was performed using two stochastic modelling functions. First, using simple weighting, when all satellites have the same weight, not taking into account the cut off elevation angle. Second, authors changed the values of the coefficients of the accepted weighting algorithm using exponential function. Based on elevation-angle the weights for phase observations were increased and at the same time weights for code observations were reduced. The calculations were compared again with the reference values as well as with values obtained from the simple weighting.

2. International GNSS service products

Created in 1994, the IGS service in its first version provided the data only for the GPS system, hence its initial name International GPS Service. With the development of other GNSS systems, its name was changed to International GNSS Service. Currently, the IGS service integrates around 200 organizations from over 80 countries (http://www.igs.org). The IGS provides, on an openly available, the highest-quality GNSS data, products and services in support of the terrestrial reference frame, Earth observation and research; positioning, navigation and timing; and other applications that benefit science and society. IGS also provide data from pilot project like: IGS-RTS and IGS-MGEX. The IGS-RTS project it is a real-time processing project especially for the PPP method and for applications requiring high accuracy in real time. It was launched officially on 1st April, 2013. MGEX, on the other hand, is designed to track, collect and analyze all available GNSS signals, both for fully operational systems as well as for emerging or regional systems.

The main data produced by IGS are created from a combined solution: Final, Rapid and Ultra-rapid, developed in postprocessing, and real-time IGS-RTS products. It is: IGS01, IGC01, IGS02 and IGS03. These products are currently only created for GPS and GLONASS systems, as they are the only fully-operational systems. In order to obtain products for all GNSS systems, MGEX data can be used. However, MGEX products are only designated by one AC and do not have a combined solution. Another source of data for PPP solutions may be one of the most active AC IGS, which is the Swiss CODE Analysis Center. Solutions from CODE are used for both combined solutions and solutions for the MGEX project.

Table 1 shows the accuracy and access time for IGS service products for GPS system.

Table 1. Official postprocessing IGS products for GPS (http://www.igs.org)

Type	Accuracy		Latency	Updates	Sample Interval
Broadcast	orbits	~ 100 cm	real time	–	daily
	Sat. clocks	~ 5 ns RMS ~ 2.5 ns SDev			
Ultra-Rapid (predicted half)	orbits	~ 5 cm	real time	at 03, 09, 15, 21 UTC	15 min
	Sat. clocks	~ 3 ns RMS ~ 1.5 ns SDev			
Ultra-Rapid (observed half)	orbits	~ 3 cm	3–9 hours	at 03, 09, 15, 21 UTC	15 min
	Sat. clocks	~ 150 ps RMS ~ 50 ps SDev			
Rapid	orbits	~ 2.5 cm	17–41 hours	at 17 UTC daily	15 min
	Sat. & Stn. clocks	~ 75 ps RMS ~ 25 ps SDev			5 min
Final	orbits	~ 2.5 cm	12–18 days	every Thursday	15 min
	Sat. & Stn. clocks	~ 75 ps RMS ~ 20 ps SDev			Sat.: 30 s Stn.: 5 min

By analyzing Table 1, it can notice that IGS provides GPS official products of: Ultra-Rapid, Rapid and Final type. Each of these products is determined by a combined solution from all ACs. They differ in accuracy and waiting time. The least accurate, but the fastest available are the Ultra-rapid products, which accuracy is 3 cm for orbit and the 150 ps for clocks, for the calculated part, and 5 cm for the orbits and 3 ns for the clocks for the predicted part. They are available with an interval of 15 min for both orbits and clocks, and the waiting time is from 3 to 9 hours (four times during each day at 3, 9, 15 and 21 of the Universal Time Coordinate (UTC) time). Much more accurate are Rapid data which have accuracy of 2.5 cm and 75 ps respectively for orbits and clocks. The waiting time is from 17 to 41 hours and the product is available with an interval of 15 min for orbits and 5 min for clocks. They are published every day at 17 UTC time. The most accurate are Final products available every Thursday. The waiting time is from 12 to 18 days. They are characterized by accuracy of 2.5 cm for orbits and 75 ps for clocks and are available with an interval of 15 min for orbits and 30 sec or 5 min for clocks.

Table 1 shows that the difference in accuracy between Rapid and Final is negligible. As described in Kouba (2015), that difference coming from the way how orbits are determined in accordance with the current conventional International Terrestrial Reference Frame (ITRF). For the calculation of IGS Rapid products, the stations forming the ITRF frame and simultaneously creating the IGS/IGb frame are held fixed along with all transformation parameters (14 parameters – geocenter, scale and orientation). This makes measurements with IGS Rapid products the most precision/consistency with the ITRF frame. However, for IGS Final products, due to the largest precision/consistency with the IGS/IGb system, geocenter and scale parameters are fixed, while orientation is not, due to the dynamics of the orbits (i.e. the gravitational field). This causes that there are small variations on the geocenter and scale parameters. These variations are determined and reported in *sinex* and *sum* files from weekly/daily solutions. From November 5, 2006, variation origin (geocenter) is included in satellite clock corrections for Final products so there should be only slight differences due to variation scale. For this reason, when taking PPP measurements with IGS Final products, to obtain the most consistent results with the current ITRF system, scale variations should be considered.

Ultra-rapid products are divided into two parts: calculated and predicted. The calculated part are determined using the data from the last 24 h, so their accuracy is much higher than those of the second part – predicted part for the next 24 hours. This is particularly true for clocks data where the accuracy differences are between 150 ps and 3 ns. This differences coming form the fact that satellite clocks do not have linear changes but are disturbed by drift and shift, which are hard to model in turn. For this reason, IGS-RTS is recommended for real time. However, they have also disadvantages in real-time casas, due to interruptions in connections (with the server, the Internet). Therefore for some real-time applications, IGS Ultra-rapid products (e.g. meteorology) are better to used (Dousa, 2001).

In this study, unofficial IGS products from the MGEX project were also used. As mentioned earlier, the MGEX project provides products for all GNSS systems that are

received from a single AC solution not like in IGS from official combined solutions. For this reason, we decided to use CODE products. The accuracy of CODE data is at the level of accuracy of official IGS products (Kouba, 2015). Until the 1961 GPS week, CODE products were made available with an interval of 15 min for orbits and 5 min for clocks, while from week 1962 these products are shared with an interval of 5 min for orbits and 5 min or 30 sec for clocks (IGSMAIL-7515).

3. Methodology

3.1. PPP model

The gLAB software, which uses the basic PPP model (also called un-differenced) was used for the conducted research. It uses non-differential observations, both code and phase, which are transformed into a linear ionosphere-free combination. The ionosphere-free linear combination is presented by the following formulas:

$$PR_3 = \alpha PR_1 + \beta PR_2\,, \tag{1}$$

$$\Phi_3 = \alpha \Phi_1 + \beta \Phi_2\,, \tag{2}$$

where: Φ_3 and PR_3 are respectively phase and code measurements of the ionosphere – free linear combination; Φ_1 are phase measurements, respectively on L_1 and L_2 expressed in meters; PR_1 and PR_2 are pseudo-range measurements, respectively L_1 and L_2; α and β, are the coefficients of the ionosphere-free linear combination which are equal to:

$$\alpha = \frac{f_1^2}{f_1^2 - f_2^2} \cong 2.545, \tag{3}$$

$$\beta = -\frac{f_2^2}{f_1^2 - f_2^2} \cong -1.545, \tag{4}$$

where: $f_1 = 1575.42$ MHz and $f_2 = 1227.60$ MHz, are respectively L_1 and L_2 frequencies.

For code and phase measurements on frequencies L_1 and L_2 error take the same value. The values adopted for our calculations are ± 2.00 m and ± 0.02 m for code and phase observations respectively. The error for the ionosphere-free linear combination can be calculated based on the dependence:

$$\sigma_{\Phi_3} = \sigma_{\Phi_1} \sqrt{(\alpha^2 + \beta^2)} \cong \pm 0.06 \text{ m}, \tag{5}$$

$$\sigma_{PR_3} = \sigma_{PR_1} \sqrt{(\alpha^2 + \beta^2)} \cong \pm 6.00 \text{ m}, \tag{6}$$

where: σ_{Φ_3} and σ_{PR_3} are errors for observing the ionosphere-free linear combination for phase and code measurements respectively.

The use of the ionosphere-free linear combination eliminates the first-order ionospheric delay. Unfortunately, the disadvantage of this combination is an increasing of noise and multipath error, as well as the not integer value ambiguity for phase measurements. The following formulas represent observational models for phase and code combinations measurements:

$$PR_3 = \rho_r^s + c\,(dt_r - dt^s) + T_r^s + e, \tag{7}$$

$$\Phi_3 = \rho_r^s + c\,(dt_r - dt^s) + T_r^s + N + \varepsilon, \tag{8}$$

where: ρ_r^s is geometric distance between the receiver and the satellite; dt_r and dt^s are corrections for the receiver and satellite clocks, respectively; T_r^s is slant tropospheric delay; N is ambiguity of the ionosphere-free linear combination; e and ε stand for other modeled and unmodeled errors, such as multipath and noise, respectively for code and phase measurements.

The gLAB software, in order to achieve high accuracy, eliminates the remaining errors and displacement effects required for the PPP method (Sanz et al., 2013): corrections of satellite orbits and clocks (through the use of precise IGS and CODE products); Phase Center Antenna (PCA = Phase Center Offset (PCO) + Phase Center Variations (PCV)) of satellite's and receiver's antenna; phase-windup for phase measurements; relativistic corrections; satellite eclipses; tidal corrections of the Earth's crust degree 2 and 3. Elimination of tropospheric delay involves modeling of the hydrostatic part of troposphere using the Simple Nominal model (Sanz et al., 2013). The remaining part, which mainly includes the wet part and the remaining non-modeled hydrostatic part, is estimated along with other unknowns. In order to reduce the number of unknowns, the tropospheric delay is determined towards the zenith, using the Niell mapping function.

The Extended Kalman Filter (EKF) filter was used to estimate the following unknowns [Yu and Gao, 2017]:

$$\delta = \left[X_r, Y_r, Z_r, c\overline{dt}_r, T_z, B_c\right], \tag{9}$$

where: X_r, Y_r and Z_r are the coordinates of the receiver; $c\overline{dt}_r$ is a correction related to the receiver clock, which also includes the code hardware delay of the receiver, multiplied by the speed of light; T_z is the estimated tropospheric zenith delay, and B_c is a new estimated parameter that, in addition to the ambiguity of the ionosphere-free linear combination includes the hardware delay of the satellite and receiver.

The process noise matrix contains stochastic models that show the values of the estimated parameters over time. For the coordinates of the receiver, we assume fixed values in time for static measurements and a random walk process for kinematic measurements. A constant value is assumed for ambiguity, unless cycle-slips are detected, then white noise is assumed. White noise is also used to adjust the receiver's clock (epoch-wise as white noise). However, for a tropospheric delay, a random walk process is assumed.

The method of determining the observation weights matrix is very important for GNSS observations. For measurements, a simple weighting $W = 1/\sigma^2$ is used where

W is weight and σ is standard deviation observation. Unfortunately, the disadvantage of such a basic weighting function is that it does not take into account the cut-off elevation angle of a satellite. Observations from low elevation mask satellites have worse accuracy than those characterized by high elevation mask satellites that pass through the thicker atmosphere layer and have greater multipath (Rotacher et al., 1998; Yu and Gao, 2017). This simple weighting was used in first calculations using Equations (5), (6) and (10).

3.2. Weighted function errors

In order to conduct further research on improving the accuracy of the PPP method, weighting function proposed by gLAB software developers was used (Equations (10) and (11)). The proposed function and its coefficient values are recommended by the MOPS standard, where this function and its coefficient is used to calculate the deviation for the multipath.

$$W = 1/\sigma^2, \tag{10}$$

$$\sigma = a + be^{-\theta/c}, \tag{11}$$

where W is the weight of the observation and σ is standard deviation, which depends on the elevation mask angle θ of a tracked satellite. Values of coefficients a, b and c are not fully appropriate, since the assumption is made that the same values are used for both code and phase observations, where $a = 0.13$ m, $b = 0.53$ m and $c = 10°$. Due to the significant difference in accuracy of phase measurements and code measurements (it is assumed that code measurements are up to 100 times less accurate), the coefficients have been modified to $a = 0.013$ m, $b = 0.053$ m for phase observations and $a = 1.3$ m and $b = 5.3$ m for code observations. Figure 1 shows the diagrams with errors obtained from

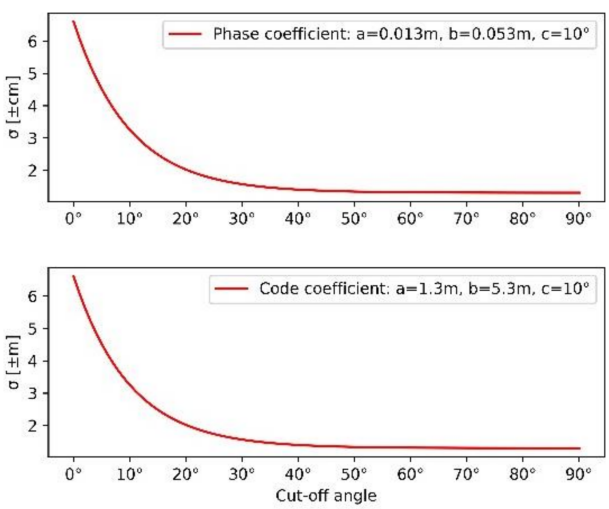

Fig. 1. Standard deviation for phase (top) and code (bottom) observation obtained from the using function depending on the cut-off elevation angle

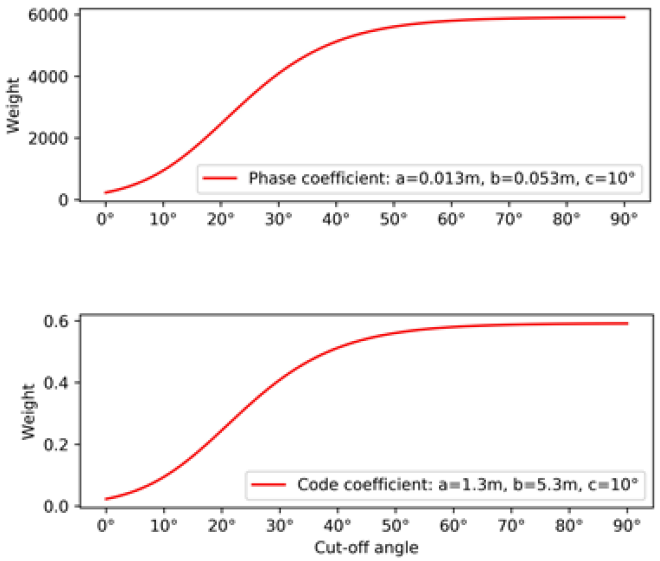

Fig. 2. Weight for phase (top) and code (bottom) observation obtained from the using function depending on the cut off elevation angle

the weighting function with proposed coefficients, while the graphs in Figure 2 show the weights depending on the cut-off elevation angle. The indicated values of coefficients a, b and c, were selected after making own tests, where for both coefficients received the best accuracy and the shortest convergence time for the analyzed stations for averaged daily results. The coefficient c remained unchanged, assuming the indicated value by the developers of the gLAB software. Values of analyzed coefficients show in Figure 3 and Figure 4.

Based on the graphs shown in Figure 1, it can be seen that the used function gives a satisfactory result. For observations from low elevation mask satellites, the error receive the largest errors, which are about ± 6.000 m for code and about ± 0.060 m for phase (for the cut off angle 0°). With the increase of the cut off angle of the satellites, the error decrease and above 70° these errors stabilize and are about ± 1.300 m for code and ± 0.013 m for the phase observations. Also on the basis of the graphs in Figure 2, one can conclude that the function used gives lower weights for low satellites and higher weights for higher elevation mask satellites. This is the desired effect, due to larger errors for low elevation mask satellites. Proposed modification of coefficients values of the weighting function, also give the desired effect, for which code observations receive much larger errors (100 times) and at the same time lower weights (10,000 times).

The same function, which was already mentioned at the end of the "Introduction", was used in the work of Gao et al. (2011), in which the coefficients were: $a = 0.003$ m, $b = 0.026$ m for phase observation and $a = 0.070$ m, $b = 0.600$ m for code observation.

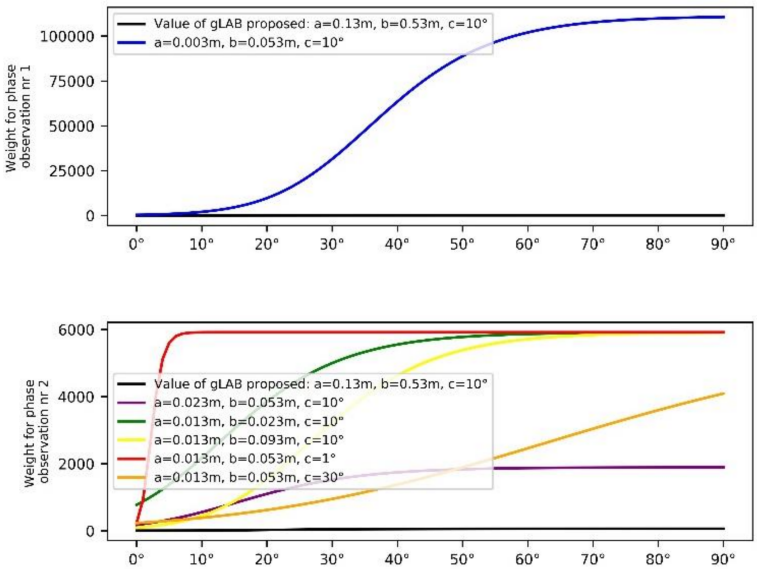

Fig. 3. Values of analyzed coefficient for exponential-function stochastic modeling for phase observation

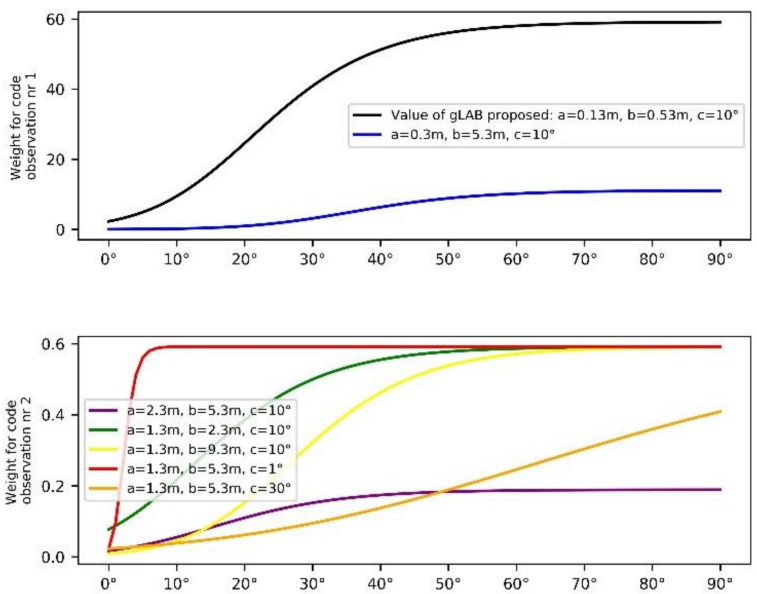

Fig. 4. Values of analyzed coefficient for exponential-function stochastic modeling for code observation

The coefficient c in both cases had a value of 20°. The use of such a proposed function resulted in a decrease in the accuracy of positioning using the PPP method as compared to simple stochastic modelling, which takes the same weights for all satellites, regardless the cut-off mask elevation angle of the satellites.

3.3. Data and solution

For the calculation of the PPP method, 4 EPN network stations have been selected which are located in Poland. The location of the selected stations and their parameters are presented in Table 2. For these stations, daily observation files were acquired with an interval of 30 sec for one day on November 25, 2017 (329 Day of Year (DOY)). The IGS products used in this case are various types of orbits (SP3 files) and clocks (CLK files). Official IGS Final, Rapid and Ultra-rapid products were obtained for orbits, with a 15-minute interval. They were obtained from a combined solution. The products calculated only by one CODE analysis center, with a 5 min interval, were also used as orbits. All GNSS products are expressed in the IGS14 reference frame. Meanwhile, official IGS Final and Rapid products were obtained as clocks, with a 5-minute interval from a combined solution, as well as clocks calculated by CODE with a 30-second interval.

Table 2. Location of selected stations along with antenna and receiver models and list of tracked GNSS systems

Station	Receiver	Antenna	Set to track GNSS	Location	
				Longitude [°]	Latitude [°]
JOZ2	LEICA GRX1200GGPRO	LEIAT504GG NONE	G+R	21.032347	52.097833
KRA1	TRIMBLE NETR5	TRM57971.00 NONE	G+R	19.920458	50.066111
LAMA	LEICA GRX1200+GNSS	LEIAT504GG LEIS	G+R	20.669937	53.892397
WROC	LEICA GR50	LEIAR25.R4 LEIT	G+R+E+C+J+S	17.062036	51.113258

The calculation parameters are presented in Table 3. The calculations were performed for each station, in 3-hour sessions on 5 solutions: FINAL, RAPID, ULTRA, CODE1 and CODE2, with the cut off angle of 3°. FINAL solution it is calculations with IGS Final products for which 15-minute orbit intervals and 5-minute clocks intervals were used. Similarly for the RAPID solution that uses IGS Rapid products. ULTRA solution it is calculations uses both orbits and clocks from Ultra-rapid products from the SP3 file, with an interval of 15 min. The other two solutions were calculated with CODE products. The first solution CODE1 uses products of both orbits as well as clocks only from the SP3 file with a 5-minute interval. Solution CODE2 uses orbits with a 5-minute interval as well as clocks with a 30-second interval.

Table 3. Processing table

GNSS	GPS
Positions	static
Input observation	daily RINEX with 30 sec observations
GNSS products with intervals and solution type	Final IGS: orbit 15 min (sp3) + clock 5 min (clk) – FINAL solution
	Rapid IGS: orbit 15 min (sp3) + clock 5 min (clk) – RAPID solution
	Ultra-rapid IGS: orbit 15 min (sp3) + clock 15 min (sp3) – ULTRA solution
	CODE: orbit 5 min (sp3) + clock 5 min (sp3) – CODE1 solution
	CODE: orbit 5 min (sp3) + clock 30 sec (clk) – CODE2 solution
Observation type	pseudorange and carrier phase on the two frequencies L1 and L2
PPP model	undifferenced PPP basic model using ionosphere-free linear combination
cut-off elevation angle	3°
reference frame	IGS14
Period	329 DOY 2017
Antenna Phase Centre – ANTEX file	igs14.atx
Stochastic model observations	pseudorange ionosphere-free error: ± 6.00 m
	carrier phase ionosphere-free error: ± 0.06 m
	weighted function:
	1) $W = 1/StDev^2$ – simple weighting
	2) $StDev = a + be^{-\theta/c}$ – weighting function
	code observations: $a = 0.13$ m, $b = 0.53$ m, $c = 10°$
	carrier phase observations: $a = 0.013$ m, $b = 0.053$ m, $c = 10°$
Ionosphere	ionosphere-free linear combination
Troposphere	hydrostatic component: Simple Nominal
	wet component: 0.1 m + estimation
Mapping function	separately for the wet and hydrostatic components – Mapping of Niell Function

4. Results

The results of the calculations made using all stations and IGS products are presented below. The accuracy and time of convergence of the determined positions as well as residual of code and phase observations were analyzed. Additionally, for selected mea-

surement sessions, an analysis also covers the errors of the XYZ ortho-cartesian coordinates and the number of satellites observed with the PDOP parameter. Then, the analysis and comparison of the obtained results were performed with the used weighting function and with the results obtained from a simple weighting.

4.1. Positioning accuracy

Figure 5 shows the average accuracy of the results obtained from all stations and from all solutions. Based on this graph, it can be seen that the accuracy of PPP positioning strongly depends on the accuracy of the GNSS products used. The best accuracy was obtained for the CODE2 solution, where the average errors of the designated positions are −2 mm, 4 mm, 9 mm, 25 mm and 32 mm, respectively for the components of ENU, horizontal (2D) and spatial (3D). FINAL, RAPID and CODE1 solution gived very similar results, which are about −5 mm, 3 mm, 10 mm, 32 mm, 41 mm for the ENU components, horizontal and spatial respectively (the differences between these solutions did not exceed 2 mm). Comparing them with results from CODE2 solution, a slight difference can be seen, where the components of the ENU are practically the same, and there are differences for horizontal and spatial, which are respectively 7 mm and 9 mm. The same

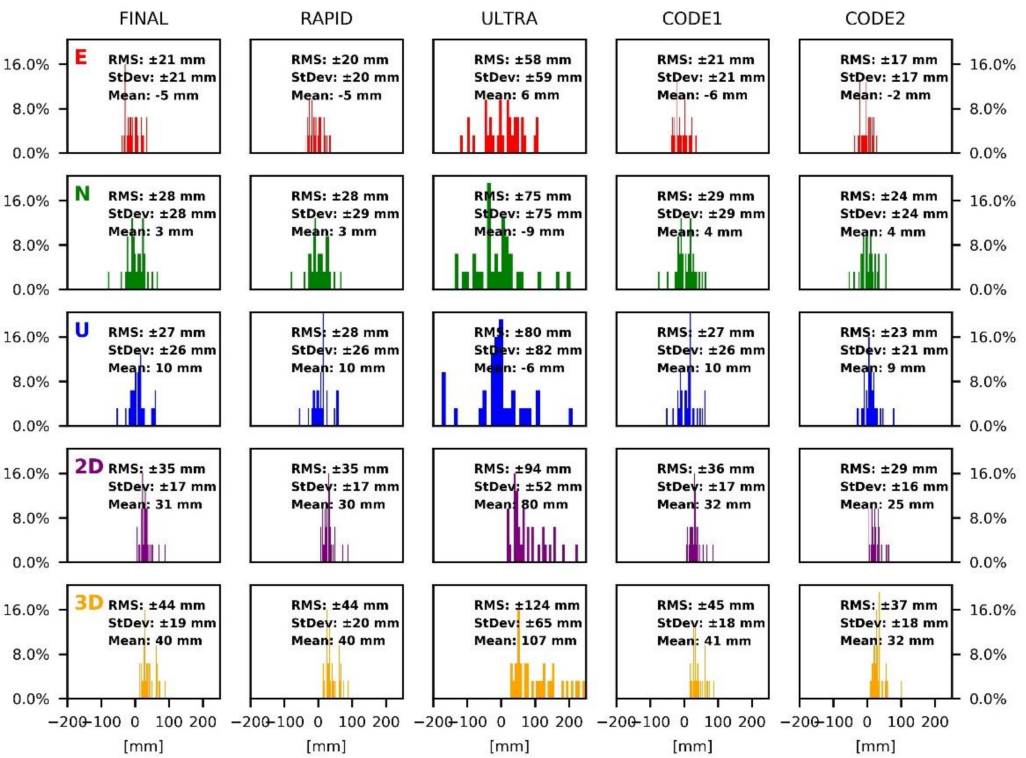

Fig. 5. Distribution of error of achieved position in topocentric coordinate for FINAL, RAPID, ULTRA, CODE1 and CODE2 solutions from all analyzed stations using three-hours dataset collected

applies to the ULTRA solution. For ENU components, a similar level of accuracy was obtained as for the CODE2 solution, and significantly larger differences for horizontal and spatial errors, respectively 80 mm and 107 mm. However, analyzing their repeatability/precision (RMS errors and standard deviation), there are significant discrepancies for ULTRA solution. This solution is characterized by RMS errors of ±58 mm, ±75 mm, ±80 mm, ±94 mm and ±124 mm for the ENU components, horizontal and spatial respectively. For the other solutions, the repeatability/precision is approximately constant at the level of ±2–3 cm for ENU components and ±3–4 cm for horizontal and spatial, again with the best results for CODE2 solution.

By analyzing the standard deviation, compared to the average ENU errors, it can be seen that the received ENU error in each case have much higher values than the standard deviation. This is due to the fact that the results obtained are very accurate, but with worse precision (all the time at the level of 1–2 cm). In case of horizontal and spatial errors it is much better – the standard deviation are smaller than the average error. It should be borne in mind that the PPP method requires a long convergence time, thus by extending the observation sessions, the precision of position determination will increase.

The results obtained depend on two elements: the accuracy and interval of IGS products (orbits and clocks). In the first case, Ultra-rapid products are the worst accuracy, especially those from the predicted part. It is precisely for them was receive the worst accuracy. Other products have very similar accuracy. In the second case, Ultra-rapid products have the longest intervals of 15 min, while FINAL, RAPID and CODE1 calculations have an interval of 5 min. The smallest data interval have CODE2 products, which is 5 min for orbit and 30 sec for clocks. The influence of the data interval is in the fact that for each observation period, it is necessary to interpolate data specific on epoch so it may produce an interpolation errors, especially for clocks. This could be the reason why accuracy and repeatability/precision for the CODE2 solution are the best along analyzed solution. The observational data and corrections of the satellite clocks in CODE2 are shared with an interval of 30 sec, so the aforementioned interpolation is not required for them.

4.2. Convergence time

Figure 6 shows the average times of convergence from all stations and from all solutions. The convergence time analyzed here is used to achieve the accuracy of determining the 3D position with an error of ±10 cm, for at least 15 min. By analyzing Figure 6, it can be seen that, just as for accuracy, the best results were obtained for the CODE2 solution, for which the convergence time was 13 min, 15 min and 12 min for E, N and U components respectively, 37 min for horizontal and 44 min for spatial. For FINAL, RAPID and CODE1 solutions significantly longer convergence times were observed (although not exceeding 2 min between each other): 20 min, 29 min, 29 min, 57 min, 71 min for the components E, N and U, horizontal and spatial respectively. The convergence times obtained are 153%, 193%, 241%, 154% and 161% worse than those for CODE2 solution. The longest convergence times were obtained for ULTRA solution: 47 min, 63 min, 49 min, 113 min and 121 min for the components E, N and U, horizontal and spatial re-

spectively, and which are respectively 361%, 420%, 408%, 305% and 275% worse than those for CODE2 solution. In addition, for ULTRA solution, it should be noted that not for all measurement session the convergence time was obtained with the assumed position accuracy of ±10 cm. For the N and U components as well as for horizontal and spatial, no convergence time was obtained for 2nd, 3rd, 4th and 11th measurement sessions, respectively. Only for the E component the convergence time of the determined position for all measurement sessions was obtained. Similarly to the accuracy of the positions determined, the convergence times obtained result from the accuracy and the interval of the IGS products used.

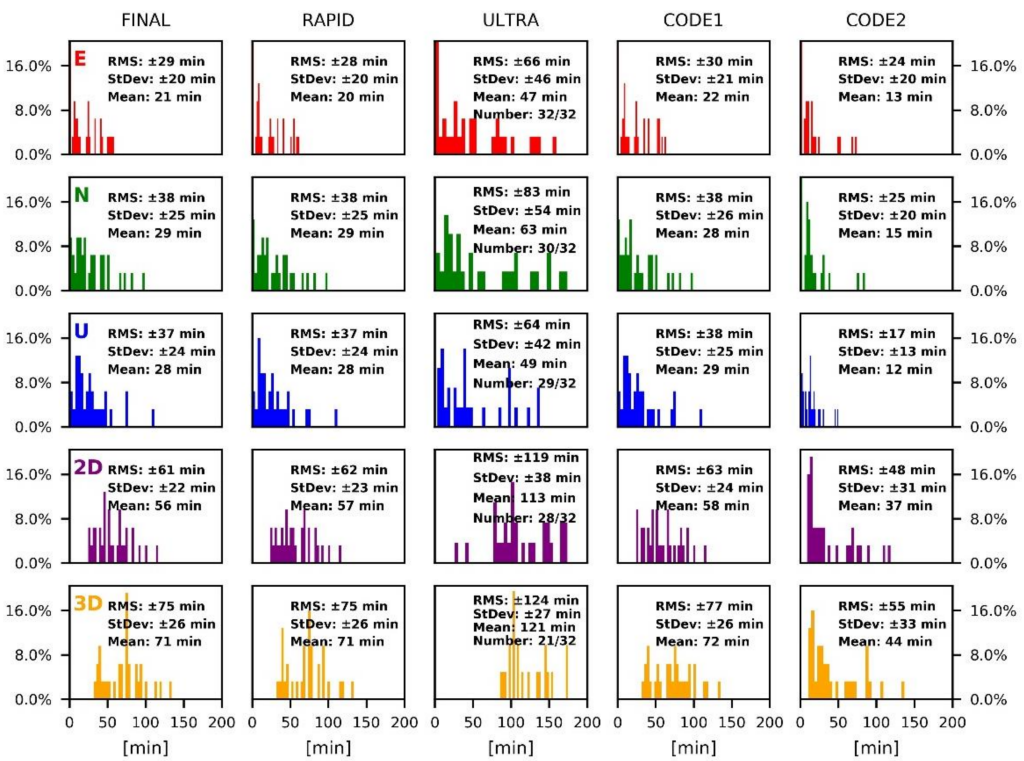

Fig. 6. Distribution of convergence time of achieved position in topocentric coordinate for FINAL, RAPID, ULTRA, CODE1 and CODE2 solutions from all analyzed stations using three-hours dataset collected

4.3. Positioning accuracy with 3 hours session

For a more detailed analysis, specific measurement sessions for each solution were analyzed. For this purpose ENU errors were analyzed. Also the number of satellites observed with the PDOP parameter as well as the formal error of ortho-cartesian coordinates for the entire measurement session from all observation epochs have been reviewed. The average ENU errors and convergence time for the entire measurement session are presented in Figures 7–11.

Figure 7 shows the results for the JOZ2 station from the observation session between 9 and 12 UTC time for the FINAL solution. The convergence time for this solution was about 41 min for spatial, while for each component of the ENU the convergence time was less than 10 min. The accuracy of the position determination was ±25 mm. Analyz-

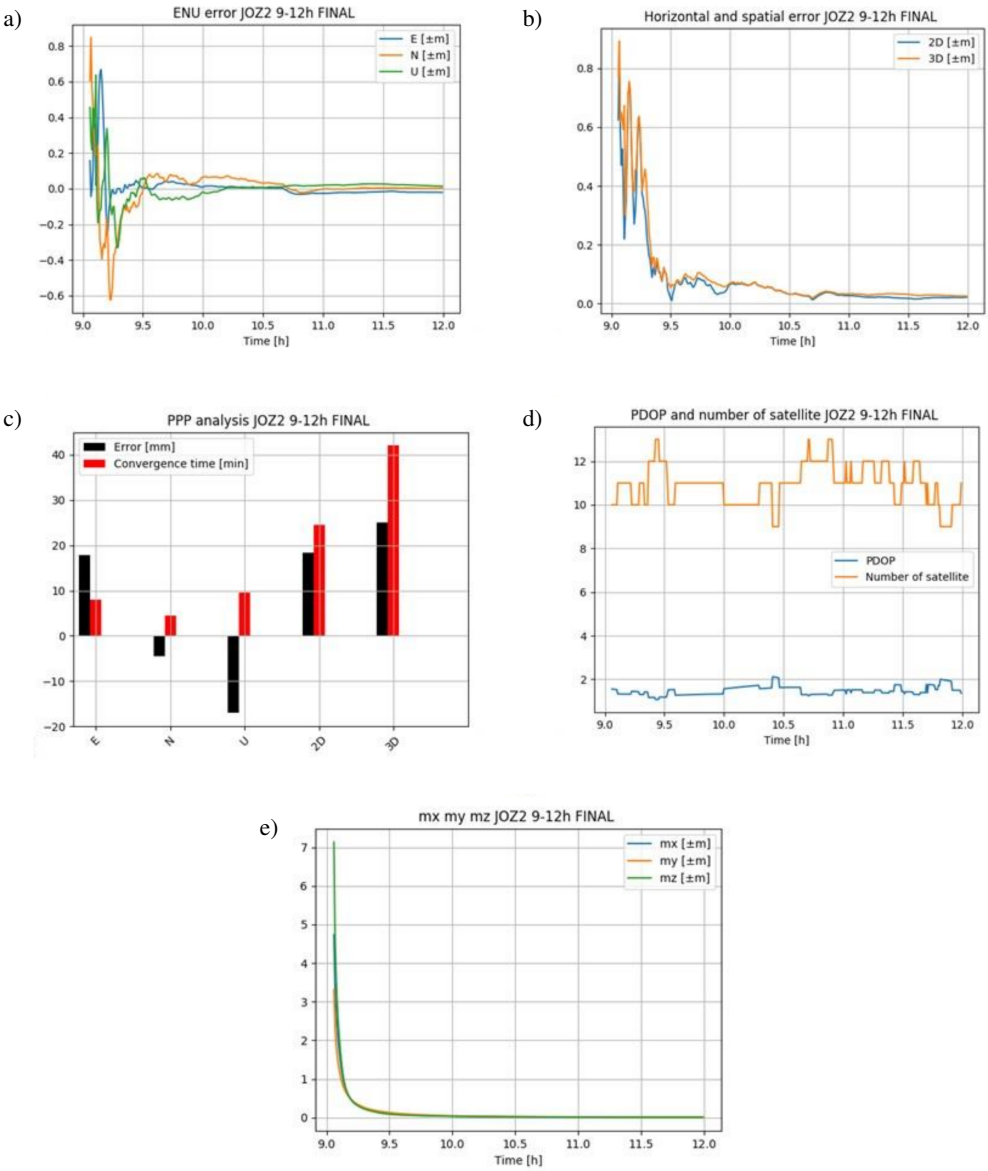

Fig. 7. PPP statistical results for JOZ2 station in three-hours period time (9–12 h in UTC) with FINAL solution. Subfigures a show error in E, N, U components. Subfigures b show horizontal (2D) and spatial (3D) error. Subfigures c show mean spatial error and convergence time with analysed period time. Subfigures d show PDOP and number of observed satellite. Subfigures e show convergence formal error XYZ coordinates

ing the graphs, it can be seen that the PPP method for the initial epochs has characteristic oscillations for each component, while after some time it stabilizes and maintains such accuracy till the end. Also for the formal error of ortho-cartesian coordinates, it can be seen that the PPP method in the initial phase is characterized by very large errors. Over time, they decrease and after a certain period of time they maintain a constant – low level. For the PPP method, the number of satellites observed also strongly influences observations. To the end, the number of satellites along with the PDOP parameter was analyzed. In this case, the number of satellites observed was on the level of 9–13 satellites, and the PDOP parameter did not exceed 2. As a result, a large number of satellites have been observed, which means that a high accuracy of PPP positioning can be achieved.

The second analyzed measurement session is for the period from 0 to 3 h for the RAPID solution (KRA1 station), shown in Figure 8. For this solution, the convergence time was 71 min, which is mainly caused by the N component, for which the convergence time was 31 min. For the U component, the convergence time was 11 min and for the E component it was 4 min. The accuracy of the position determination for this solution was ±41 mm. By analyzing the course of error, it can be seen that for this solution, the initial error are very large, especially for the N component. This is most likely due to the

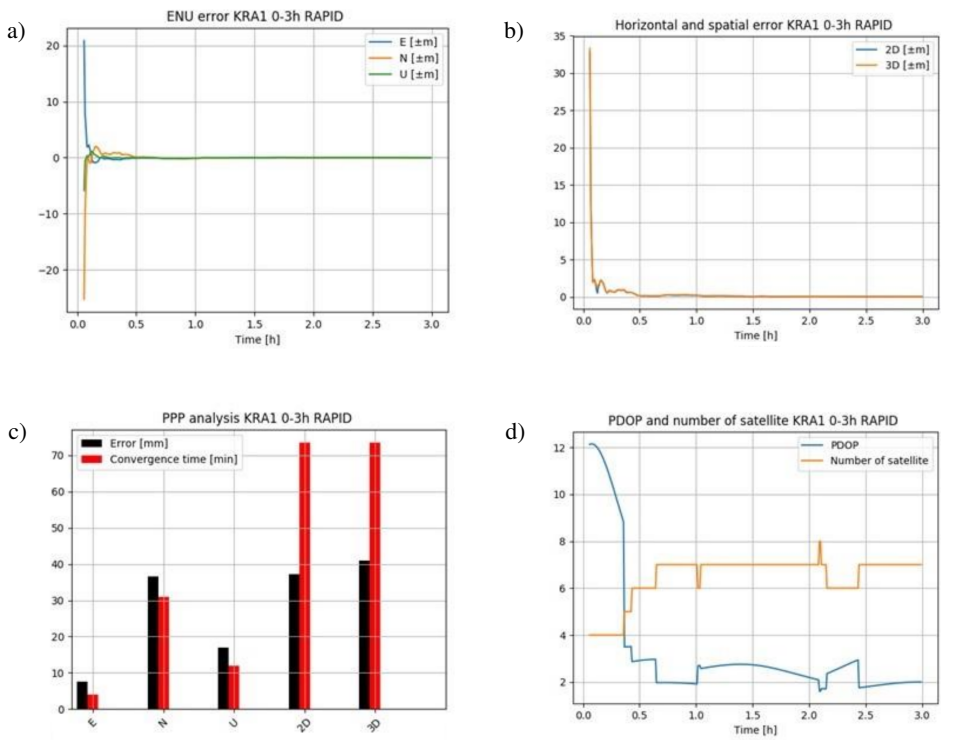

Fig. 8. PPP statistical results for KRA1 station in three-hours period time (0–3 h in UTC) with RAPID solution. Subfigures a show error in E, N, U components. Subfigures b show horizontal (2D) and spatial (3D) error. Subfigures c show mean spatial error and convergence time with analyzed period time. Subfigures d show PDOP and number of observed satellite

number of satellites observed, where for the first 25 min only 4 satellites were observed. It was only after about 30 min that the number increased to 6 satellites, and then to 7 satellites with selected epochs, where 6 or 8 satellites were observed.

The third analyzed session, shown in Figure 8, is for hours 21–24 h for ULTRA solution (LAMA station). For this solution, despite the large number of satellites observed, the positioning accuracy was ±22.5 cm. The convergence time was not obtained in this case. Convergence was observed for horizontal and it was 150 min and the E, N and U components was respectively 130 min, 5 min and 105 min. Analyzing graphs 6a and 6b, it can be seen that it was only after about 2 hours that the accuracy of positioning fell below ± 25 cm, while for the first hour it was above 1 m. The number of satellites observed over the entire period did not decrease below 8 satellites, and the PDOP parameter did not exceed 2. Based on the above analysis, it can be concluded that the results obtained relate with the accuracy of the GNSS products used. Ultra-rapid IGS products were used for this solution. For the second 12 hours (hours 12 to 24 UTC time) the products are from the prediction stage, where their accuracy is much lower, especially for clocks. This might be the reason for the results obtained.

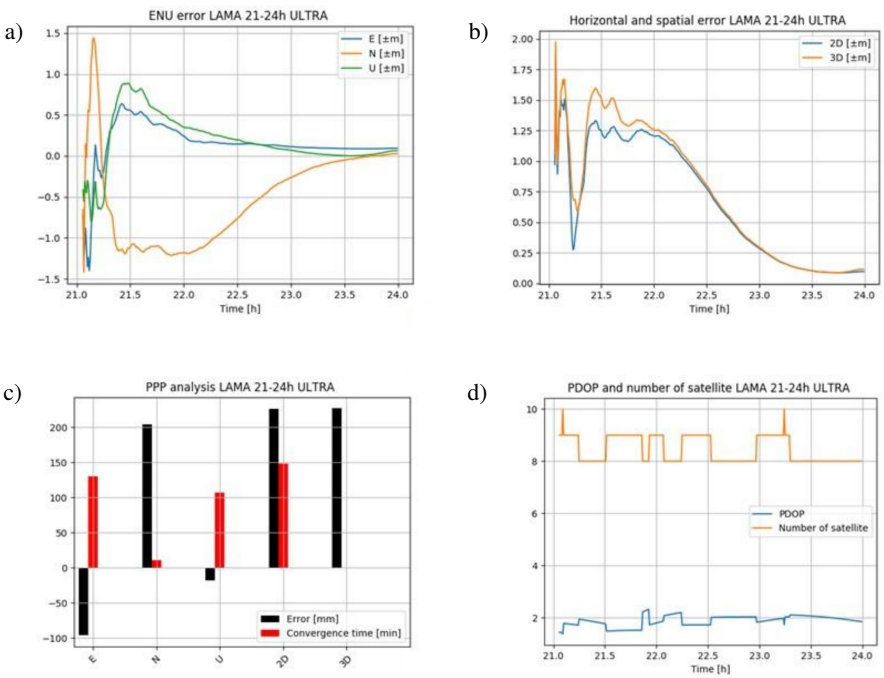

Fig. 9. PPP statistical results for LAMA station in three-hours period time (21–24 h in UTC) with ULTRA solution. Subfigures a show error in E, N, U components. Subfigures b show horizontal (2D) and spatial (3D) error. Subfigures c show mean spatial error and convergence time with analyzed period time. Subfigures d show PDOP and number of observed satellite

The other two analyzed measurement sessions are calculations using CODE products. In Figure 10, the analysis for the CODE1 solution for the WROC station, (hours

from 15 to 18 UTC time) is presented. In this measurement session, the convergence time was 57 min. By analyzing the convergence time for each component, it can be seen that the N component had a significant influence. For this component, the convergence time was over 52 min, where for the remaining components, it did not exceed 15 min. The position accuracy is ±54 mm, with the number of satellites observed between 8 and 12 (PDOP parameter below 2, except 15 min after 17 UTC time, where PDOP increased slightly but did not exceed 2.5). Figure 11 shows the analysis of the measurement session for the CODE2 solution for WROC stations (hours between 21 and midnight). Convergence time was one hour, with a position error of ±57 mm. For this solution, the component E, for which the convergence time was 50 min and the error −38 mm had the greatest impact on the convergence time and accuracy. A somewhat surprising effect is the fast convergence time for the U component, which was 2 min, but the error was 40 mm. In most measurement sessions, this U component has the longest convergence time and the biggest error. For the N component, the convergence time was 27 min, with the least error of 8 mm. Analyzing the number of satellites observed, it can be seen that the closer to the midnight the more the number of satellites decreases. Between 21 and 22 h the number of visible satellites is from 10–12, while after 22 h there are 8–9 satellites observed. Along with the decreasing number of satellites, the PDOP parameter increases (for hour 21 h it was 1.5, and after 23 h PDOP was 2).

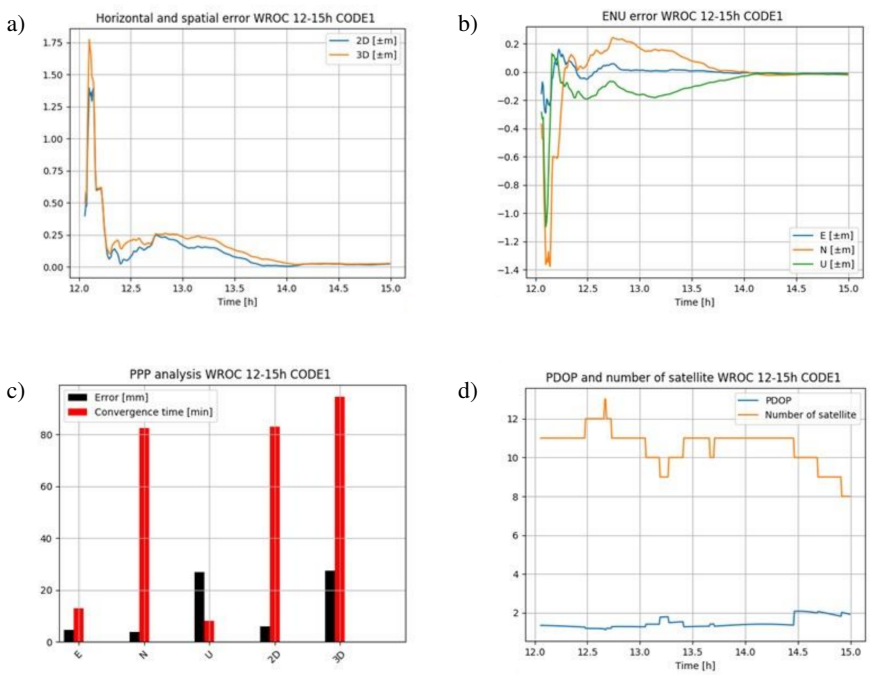

Fig. 10. PPP statistical results for WROC station in three-hours period time (15–18 h in UTC) with CODE1 solution. Subfigures a show error in E, N, U components. Subfigures Index b show horizontal (2D) and spatial (3D) error. Subfigures c show mean spatial error and convergence time with analyzed period time. Subfigures d show PDOP and number of observed satellite

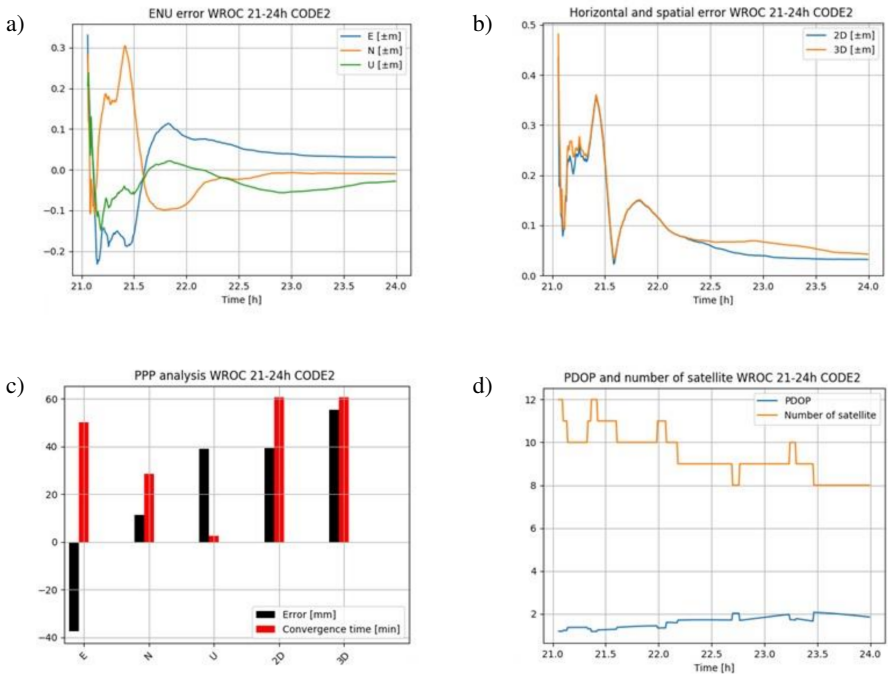

Fig. 11. PPP statistical results for WROC station in three-hours period time (21–24 h in UTC) with CODE2 solution. Subfigures a show error in E, N, U components. Subfigures b show horizontal (2D) and spatial (3D) error. Subfigures c show mean spatial error and convergence time with analyzed period time. Subfigures d show PDOP and number of observed satellite

4.4. Residual analysis

Another analysis demonstrating the accuracy of the PPP method it is the analysis of residual of the used ionosphere-free linear combination. Residual may indicate the precision of measurements as well as the quality of observation modeling. Based on it, one can determine if there are any unmodeled, systematic or gross errors, e.g. cycle-slips. Figures 12–13 show residual for phase and code observations respectively.

By analyzing Figure 12 it can be seen that the smallest residual for phase observations were obtained for the CODE2 solution for each station. In that solution, the RMS is approximately ± 1 cm and the range is from -5 mm to 5 mm. Slightly larger spread of residuals of phase observations is for the remaining solutions, in addition to the ULTRA solution. The variation for these solutions ranges from -2 cm to 2 cm, while the RMS are around ± 3 cm. The largest residuals were obtained for the ULTRA solution, for which the RMS are respectively: ± 3.9 cm for KRA1 station, ± 4.5 cm for JOZ2 and LAMA stations and ± 4.7 cm for WROC station. The variation of residuals ranges in the same way as solutions FINAL, RAPID and CODE1, but with a much larger oscillation. In addition, the residual have the highest at the end of the day, which is due to the prediction of orbits. Also for the JOZ2 station, it can be seen that there is one sig-

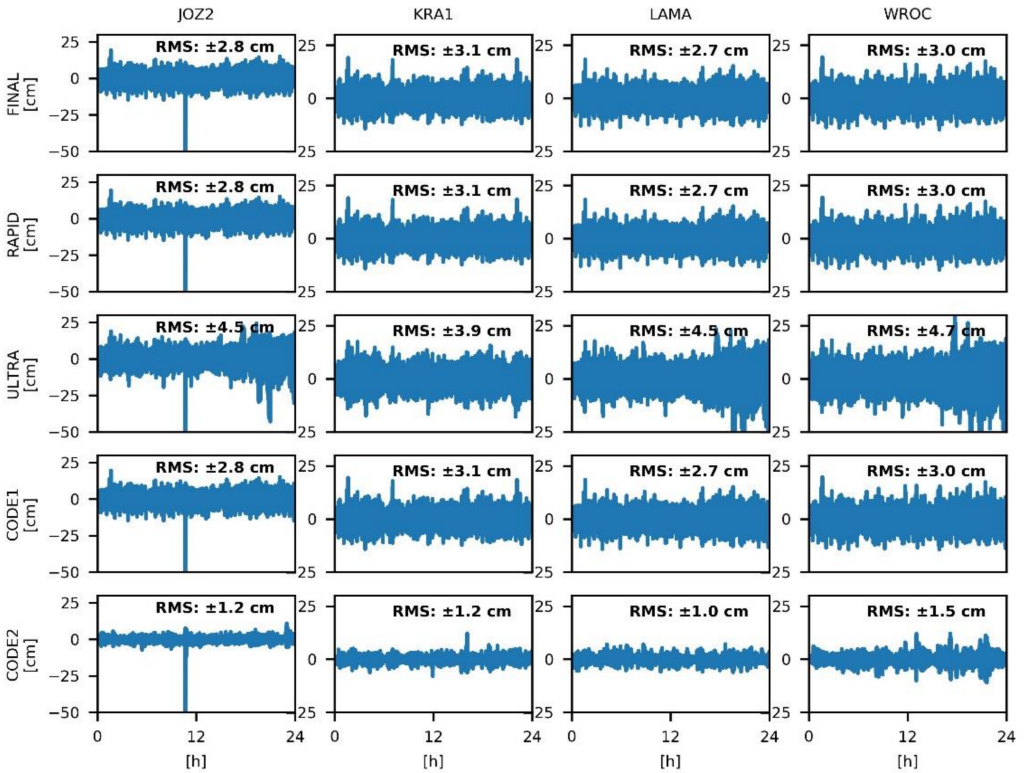

Fig. 12. Residuals phase observations for FINAL, RAPID, ULTRA, CODE1 and COED2 solution for all analyzed stations

nificant residual that goes beyond the graph. It most likely results from an unnoticed cycle-slip.

By analyzing Figure 13, it can be noticed that the residual for code observations are not dependent on the products used, but on the station itself. For each station and for each solution virtually the same residual were obtained. The smallest residual were obtained for WROC station, where the range is from –1.5 m to 3 m, with RMS ± 1 m. Similar residuals were obtained for JOZ2 and LAMA stations: from -5 m to 5 m with RMS respectively ± 1.3 m and ± 1.2 m. The highest residual were obtained for the KRA1 station, in the range of -20 m, up to 20 m, with RMS ± 2.4 m.

Analyzing the above results, it can be seen that the residual for code observations are strongly dependent on the type of receiver used (Table 2). Each type of antenna receiver has its own clock, and this has a significant impact on pseudorange measurements. The smallest residual for code observations are for WROC station. This station, compared to the others, has the newest type of LEICA GR50 receiver, which first appeared at stations in 2016. Slightly lower residuals are for JOZ2 and LAMA stations, which have a similar - slightly older types of receivers: LEICA GRX1200GGPRO and LEICA GRX1200 + GNSS respectively, which were established at points in 2007 and

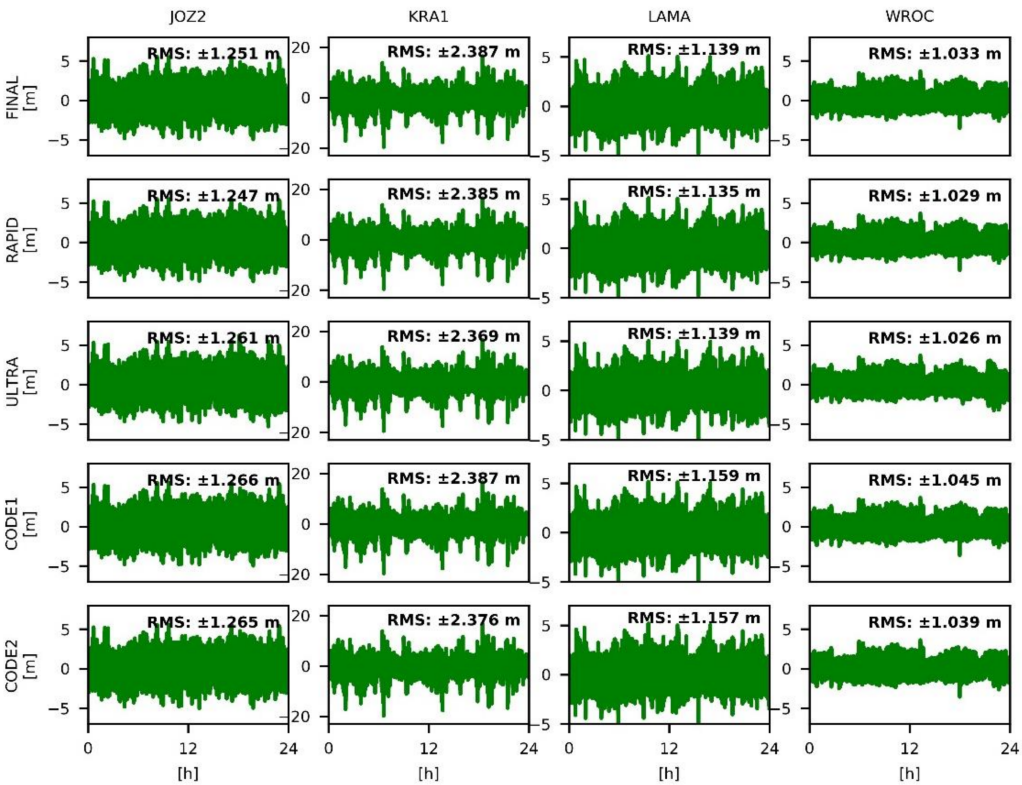

Fig. 13. Residuals code observations for FINAL, RAPID, ULTRA, CODE1 and COED2 solution for all analyzed stations

2009 respectively. The largest residuals were obtained for the KRA1 station. This station, compared to the others, has the oldest type of the receiver among the stations taken into account in the research – TRIMBLE NETR5 (first appeared in 2006). It should be mentioned, however, that the residual do not only depend on the receiver used, as it was shown above.

4.5. Results with weighted function

In order to check the accuracy of the used weighting function, errors, time of convergence of the determined positions and residual for phase and code observations were compared with the values obtained from the simple weighting. The results of the analyzes performed are presented in Figures 14–17. Analysis were covered the error between the simple weighting and the used function (Figure 14). An improvement in accuracy for calculations with IGS Final and Rapid products for each solution with the weighting function used can be observed. Error lowered by about 30% for the components of the ENU and by about 15% for the horizontal and spatial ones. The mean error for ENU components do not exceed 5 mm and for horizontal and spatial they are approx-

imately 3 cm. Also, when analyzing the standard deviation and RMS, an improvement of 15% can be noticed. For IGS Ultra-rapid products, the difference for the E and N components is better for weighting function (4 mm and −4 mm respectively), compared to the results with a simple weighting (6 mm and −9 mm respectively). However, when analyzing the standard deviation and RMS for Ultra-rapid products, larger values were obtained, especially for the E component, increasing up to ±6 cm and ± 8 cm. For the U, horizontal and spatial, U components worse results were obtained using the weighting function, especially for horizontal and spatial. The differences between them are respectively 5 mm, 12 mm and 15 mm. Also for horizontal and spatial, the standard deviation and RMS have increased by approximately ±2 cm.

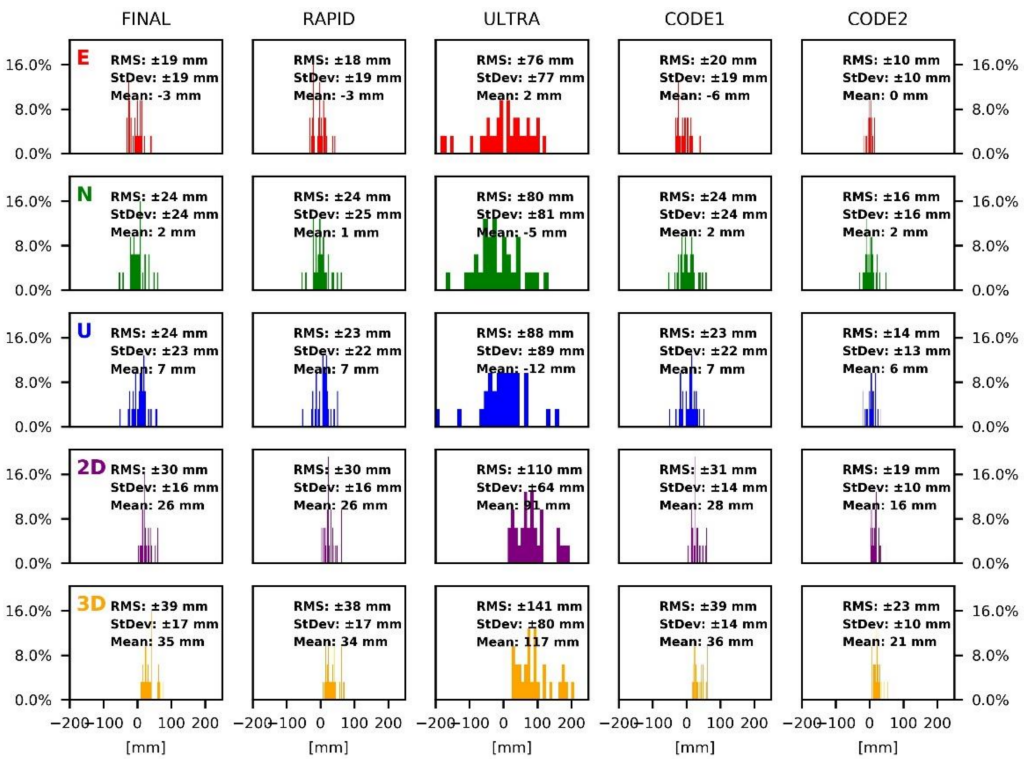

Fig. 14. Distribution of error of achieved position in topocentric coordinate for FINAL, RAPID, ULTRA, CODE1 and CODE2 solutions from all analyzed stations using three-hours dataset collected with weighted function

Using the CODE products (CODE1 and CODE2 solutions), for calculations with the weighting function, improved the accuracy for each analyzed error. Difference for horizontal components E and N did not exceed 2 mm, while for the U component, the difference was equal to 3 mm. Significant differences were observed for horizontal and spatial, which are respectively 4 mm (CODE1) and 9 mm (CODE2) for horizontal and 5 mm (CODE1) and 11 mm (CODE2) for spatial. Analyzing the standard deviation and RMS for CODE1 solution, the differences between the simple weighting and the

used function one did not exceed ±5 mm. For CODE2 solution, much larger differences were obtained in terms of accuracy: respectively: ±7 mm, ±8 mm, ±7 mm, ±10 mm, ±10 mm for the components of ENU, horizontal and spatial, respectively.

Summarizing above, it can be seen that the use of the weighting function improves the accuracy for each product used. The only exception here are Ultra-rapid products. Particularly the improvement is seen for calculations with CODE2 products for which the best results were obtained – the error were 0 mm, 2 mm, 5 mm, 16 mm and 21 mm, respectively for ENU and horizontal and spatial. For these calculations very high precision was also obtained (the standard deviation and RMS errors are below ±2 cm).

Taking into account the convergence times (Figure 15), the differences between the simple weighting and the used weighting function, can be seen. Using the weighting function, the longer convergence times appears, but at the same time the maximum difference between them did not exceed 5 min (with a predominance of 1–2 min). The exception are convergence times for calculations with CODE2 products, for which the difference between them did not exceed 1 min for the components of the ENU, and a significant improvement was obtained for horizontal and spatial. For horizontal, the dif-

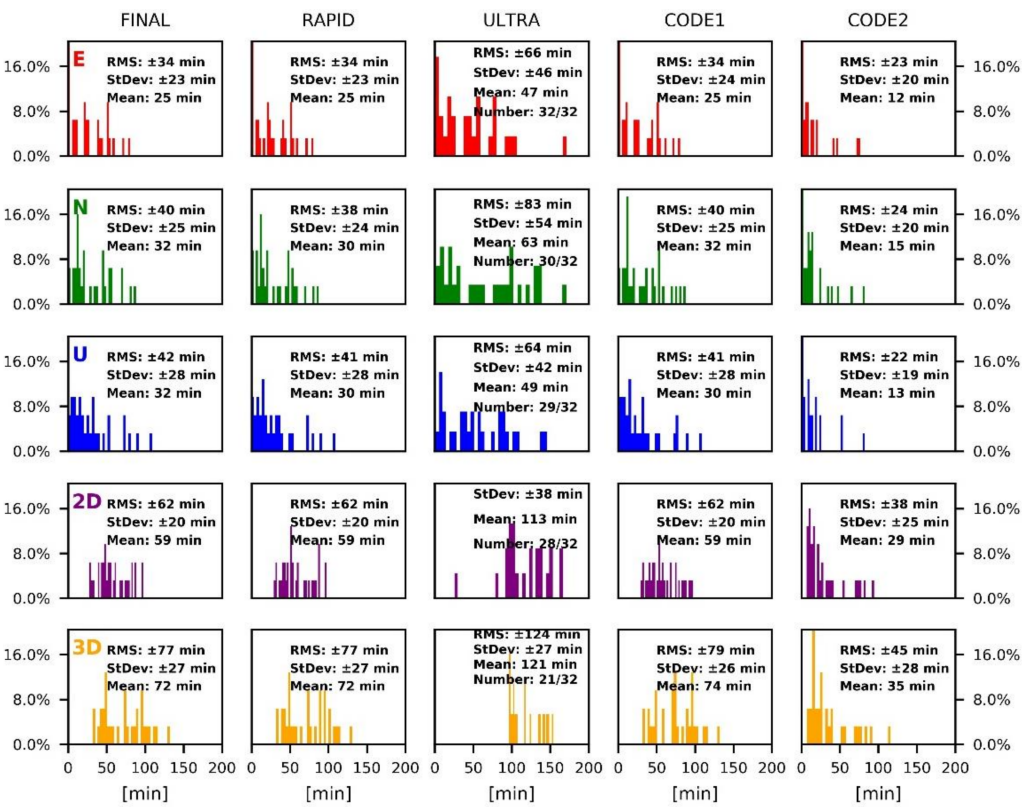

Fig. 15. Distribution of convergence time of achieved position in topocentric coordinate for FINAL, RAPID, ULTRA, CODE1 and CODE2 solutions from all analyzed stations using three-hours dataset collected with weighted function

ference was 8 min (22%) and for spatial 9 min (21%). Similar applications were received for standard deviation and RMS.

For ULTRA solution, the time of convergence of the determined position with the assumed error of ±10 cm was not obtained for every measurement session. When comparing the number of convergence times obtained with the number obtained from calculations with a simple weighting a smaller number of measuring sessions with convergence were observed. For the E component no convergence of the determined position was obtained for 3 measurement sessions, while all convergence times were for a simple weighting. For horizontal and spatial, respectively, by 5 and 2 measurement sessions less.

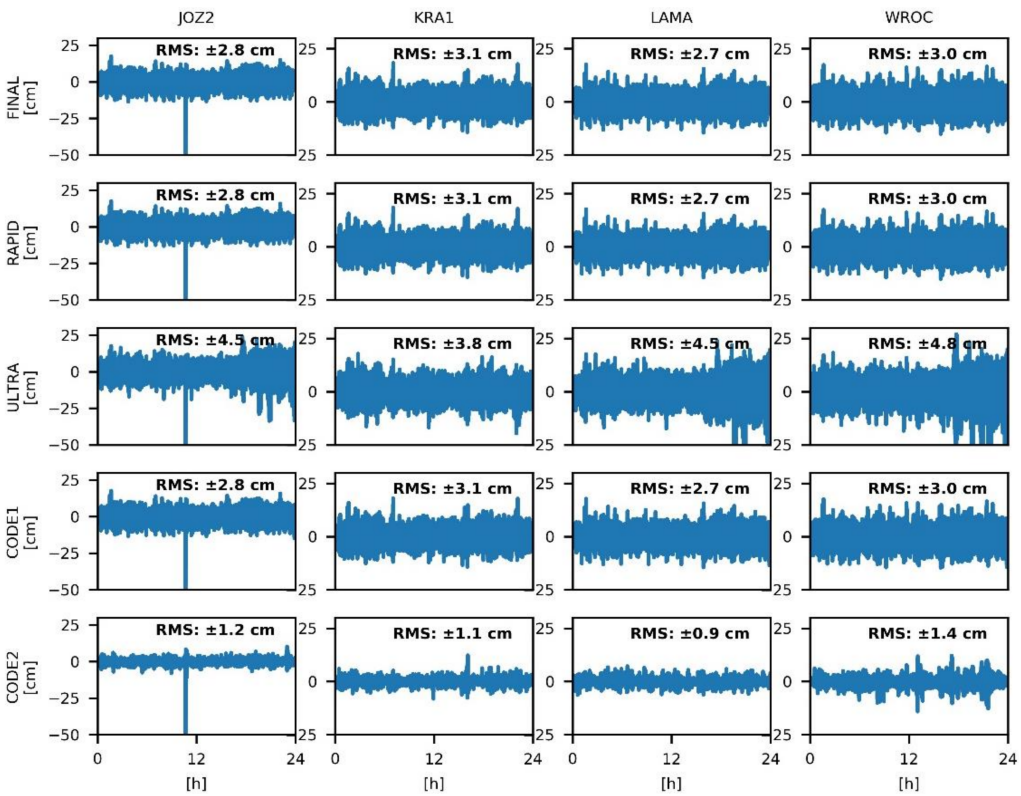

Fig. 16. Residual value phase observations for FINAL, RAPID, ULTRA, CODE1 and CODE2 solution for all analyzed stations with weighted function

Additionally, in order to determine the assessment of the weighting function, residual, presented in Figures 16 and 17, were also calculated. Comparing residual RMS with values from a simple weighting, gives practically no difference. For phase observations, the occurring differences in RMS are 1 mm, while for code measurements the differences do not exceed 3 cm, which in terms of required accuracy of code measurements do not affect the obtained results.

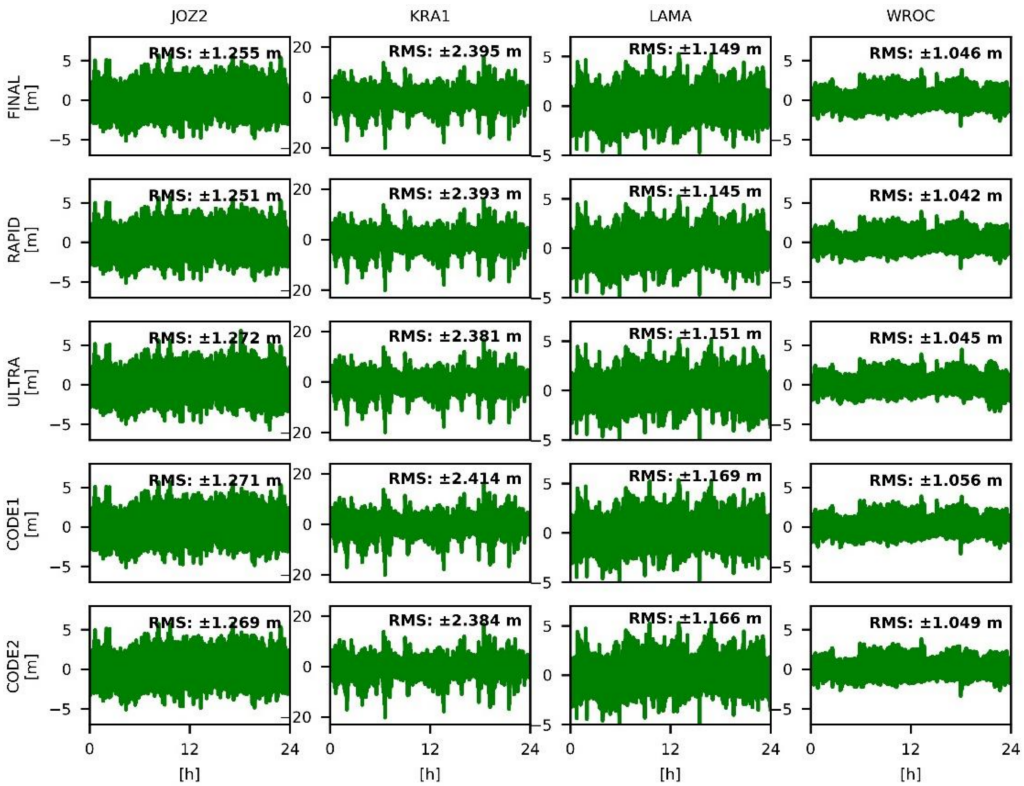

Fig. 17. Residual value code observations for FINAL, RAPID, ULTRA, CODE1 and CODE2 solution for all analyzed stations with weighted function

5. Discussion

The research carried out by the authors were focused on the analysis of the PPP positioning accuracy, using various GNSS products, for calculations only with the GPS system. For this purpose, the positions of 4 EPN network stations from 3-hour measurement sessions were analyzed for one day, along with the convergence time of the determined position using IGS products: Final, Rapid, Ultra-rapid and CODE. The used products are characterized by different accuracy. Besides, the Final, Rapid and Ultra-rapid products are obtained from the IGS combined solution, while the CODE products are calculated only by one AC (Kouba, 2015). The data used is also characterized by different intervals, which affects the accuracy of interpolation, especially for clock corrections (Nistor and Buda, 2016).

From the results obtained, it can be seen that the best accuracy and the shortest convergence time were observed for the CODE2 solution. The highest precision was also obtained for these calculations. The products used in these solutions had the smallest data interval, in particular corrections to the satellite clocks, which were at a 30 sec interval, which is the same as the interval for determining the position. Thanks to this,

interpolation of clocks was not required. Calculations of FINAL, RAPID and CODE1 solutions were characterized by very similar results, despite the fact that the used Final and Rapid products had orbits with a 15 min interval, while the products used for CODE1 solution had orbits with a 5 min interval. For these solutions, the clocks were with a 5 min interval, received from CLK files, in addition to CODE1, where corrections to the satellite clocks were read from the SP3 file. The worst accuracy and the longest convergence time were for ULTRA solutions, in particular for the second half of the day, where the orbits and clocks are predicted. Ultra-rapid products are shared in the form of SP3 files with a 15 min interval, which contain both orbits and corrections to satellite clocks. For these calculations about 66% of convergence times were obtained with the assumed accuracy of position determination of ± 10 cm.

Analyzing the differences between CODE1 solution and CODE2 solution, shows that the accuracy and precision of PPP positioning have a big impact on satellite clocks. For these calculations, the same orbits but different corrections to satellite clocks (different intervals) were used. For CODE1, corrections was read from the SP3 file, while for CODE2 they were corrections read from the CLK file. Analysis of the accuracy of PPP positioning depending on the interval of corrections to satellite clocks as it was carried out in the works of Guo et al., 2010 and Hesselbarth and Wanninger 2008, in which similar dependencies were obtained.

Subsequent studies concerned the method of stochastic modeling of observations. As it is shown in the works of Kaźmierski et al., 2018, Yu and Gao, 2017, proper weighting of observations have a big impact on the accuracy of PPP positioning. In the first method, a simple weighting is used that accepts the same errors for code and phase observations for each satellite. The second function, on the other hand, performs the weighting of observations, depending on the satellite elevation mask angle, where low satellites take much lower weights than those with a high elevation mask. When comparing the obtained results, it can be seen that the inclusion of the elevation angle of the satellites improved the results. Both accuracy and precision in all solutions have improved, apart from ULTRA, where slightly worse results was obtained. In particular, the results for CODE2, mainly precision, have improved. Analyzing the times of convergence, the use of the weighting function resulted in a longer coincidence time of the determined position, except for CODE2 solutions. However, the differences between them is insignificant. For CODE2 the convergence time for horizontal and spatial errors has been significantly reduced, which again confirms the correctness of the used weighting function.

The same function was used in the work of Gao et al., 2011. However, in these studies other values of coefficients were adopted, which resulted in poorer accuracy. Comparing the obtained results of the author's calculations, with the mentioned work, it was shown that appropriate stochastic modeling can improve the accuracy of PPP positioning, using the same functions.

By analyzing the received precision, it can be seen that standard deviations are greater than ENU errors. This is mainly due to long convergence times and short measuring sessions of 3 hours. By prolonging the observation sessions, it is expected that the precision and accuracy will increase.

Finally analysis it was review of the residual of phase and code observations. Generally, the residual of phase observations depend on the products used. Again, the best results were obtained for CODE2 and the worst for ULTRA. However, the residual of code observations depend on the type of receiver used (the clock oscillator). The older the receiver model, the higher the residual were obtained, in contrast to the newest receiver, for which the lowest residual were obtained.

6. Conclusion

Based on the results obtained, it can be concluded that the best accuracy was obtained for the CODE2 calculation. They were characterized by the highest accuracy and precision as well as the shortest convergence time. Also, the application used weighting function, including the elevation mask angle, resulted in accuracy improvements. The time of convergence of the position determination by 21% (9 min) was significantly reduced compared to the simple weighting. The results accuracy were of several mm for each ENU component and less than 2 cm for the determined 3D position, with a convergence time of about 40 min. The worst results were obtained for ULTRA calculations, for which a position with assumed accuracy was not obtained for none of the measurement sessions. The use of the weighting function for these calculations slightly downgrade the results and increased the time of convergence. The accuracy for these calculations were around 10 cm, with a convergence time of 2 hours. For the remaining calculations, with FINAL, RAPID and CODE1 data, were very similar results. Accuracy for these calculations was about 3.5 cm, with a convergence time of about 70 min. For these calculations, the use of the weighting function resulted in increased accuracy and also reduced convergence time. It should be emphasized that in this case the differences were negligible.

Finally, it can be concluded that the PPP method for static positioning allows to achieve high accuracy of position determination. The results depend to a large extent on the IGS products used and their intervals, especially corrections to satellite clocks. Also, a large influence on the obtained results is due to the stochastic modeling of observations and the type of the receiver, especially if pseudorange measurements are used.

Acknowledgement

This work was supported by the Faculty of Civil Engineering and Geodesy, Institute of Geodesy of the Military University of Technology with the statutory research funds.

References

Afifi, A. and El-Rabbany, A. (2016). Improved Between-Satellite Single-Difference Precise Point Positioning Model Using Triple GNSS Constellations: GPS, Galileo, and BeiDou. *Positioning*, 7, 63–74. DOI: 10.4236/pos.2016.72006.

Ahmed, F., Václavovic, P., Teferle, F.N., Dousa, J., Bingley, R.M. and Laurichesse, D. (2016). Comparative analysis of real-time precise point positioning zenith total delay estimates. *GPS Solutions*, 20(2), 187–199. ISSN 1521-1886.

Banville, S., Sieradzki, R., Hoque, M., Wezka, K. and Hadas, T. (2017). On the estimation of higher-order ionospheric effects in precise point positioning. *GPS Solut.*, 1–12. DOI: 10.1007/s10291-017-0655-0.

Bałdysz, Z., Nykiel, G., Figurski, M. and Araszkiewicz, A. (2108). Assessment of the Impact of GNSS Processing Strategies on the Long-Term Parameters of 20 Years IWV Time Series. *Remote Sens.*, 10, 496.

Cai, C. et al. (2015). Precise point positioning with quad-constellations: GPS, BeiDou, GLONASS and Galileo. *Adv. Space Res*. DOI: 10.1016/j.asr.2015.04.001.

Collins, P., Bisnath, S., Lahaye, F. and Heroux, P. (2010). Undifferenced GPS Ambiguity Resolution Using the Decoupled Clock Model and Ambiguity Datum Fixing. *Journal of Navigation*, 57(2), 123–135.

Cerretto, G., Tavella, P., Lahaye, F., Mireault, Y. and Rovera, D. (2012). Near realtime comparison and monitoring of time scales with Precise Point Positioning using NRCan Ultra-Rapid Products. *IEEE Trans. Ultrason. Ferroelectr. Freq. Control*, 59(3), 545–551.

Dousa, J. (2001). The Impact of Ultra-Rapid Orbits on Precipitable Water Vapor Estimation using Ground GPS Network. *Physics and Chemistry of the Earth, Part A: Solid Earth and Geodesy*, 26(6-8), 393–398.

Dousa, J. and Vaclavovic, P. (2014). Real-time zenith tropospheric delays in support of numerical weather prediction applications. *Adv Space Res*, 53(9), 1347–1358. DOI: 10.1016/j.asr.2014.02.021.

Elsobeiey, M. and El-Rabbany, A. (2013). An Efficient Precise Point Positioning Model for Near Real-Time Applications. *Proceedings of the 2013 International Technical Meeting of The Institute of Navigation*, San Diego, California, January 2013, pp. 318–324.

Elsobeiey, M. and El-Rabbany, A. (2014). Efficient Between-Satellite Single-Difference Precise Point Positioning Model. *Journal of Surveying Engineering*, 140(2), 04014007. DOI: 10.1061/(ASCE)SU.1943-5428.0000125.

Gao, C., Wu, F., Chen, W. and Wang, W. (2011). An improved weight stochastic model in GPS Precise Point Positioning. *Proceedings of the 2011 International Conference On Transportation, Mechanical, and Electrical Engineering (TMEE)*, Changchun, China, 16–18 December 2011.

Ge, M., Gendt, G., Rothacher, M., Shi, C. and Liu, J. (2008). Resolution of GPS carrier-phase ambiguities in Precise Point Positioning (PPP) with daily observations. *J. Geod.* DOI: 10.1007/s00190-007-0187-4.

Ge, Y., Zhou, F., Sun, B., Wang, S. and Shi, B. (2017). The Impact of Satellite Time Group Delay and Inter-Frequency Differential Code Bias Corrections on Multi-GNSS Combined Positioning. *Sensors* (Basel, Switzerland), 17(3), 602. DOI: 10.3390/s17030602.

Geng, J., Bock, D., Melgar, B., Crowell, W. and Haase, J.S. (2013). A new seismogeodetic approach applied to GPS and accelerometer observations of the 2012 Brawley seismic swarm: Implications for earthquake early warning. *Geochem. Geophys. Geosyst.*, 14, 2124–2142. DOI: 10.1002/ggge.20144.

Gołaszewski, P., Wielgosz, P. and Stępniak, K. (2017). Intercomparison and validation of GNSS-IWV derived with G-Nut and Bernese software. Proceeding paper: *The 10th International Conference "Environmental Engineering"*, 27-28 April 2017, Vilnius, Lithuania.

Grejner-Brzezinska, D.A., Kashani, I. and Wielgosz, P. (2005). On accuracy and reliability of instantaneous network RTK as a function of network geometry, station separation, and data processing strategy. *GPS Solut*, 9, 212–225.

Guo, F., Zhang, X., Li, X. and Cai, S. (2010). Impact of sampling rate of IGS satellite clock on precise point positioning. *Geo-spat. Inf. Sci.*, 13(2), 150–156. DOI: 10.1007/s11806-010-0226-9.

Hadaś, T., Kaplon, J., Bosy, J., Sierny, J. and Wilgan, K. (2103). Near-real-time regional troposphere models for the GNSS precise point positioning technique. *Meas. Sci Technol*.

Han S. (1997). Quality Control Issues Relating to Instantaneous Ambiguity Resolution for Real-time GPS Kinematics Positioning. *Journal of Geodesy*, 71, 351–361. DOI: 10.1007/s001900050103.

Hesselbarth, A. and Wanninger, L. (2008). Short-term stability of GNSS satellite clocks and its effects on Precise Point Positioning. *Proc. ION GNSS*, Savannah, Georgia, 16-19 September, 1855–1863.

Hoechner, A., Ge, M., Babeyko, A.Y. and Sobolev, S.V. (2013). Instant tsunami early warning based on real-time GPS-Tohoku 2011 case study. *Nat. Hazards Earth Syst. Sci*, 13, 1285–1292. DOI: 10.5194/nhess-13-1285-2013.

Hofmann-Wellenhof, B., H. Lichtenegger and Wasle, E. (2008). *GNSS-Global Navigation Satellite System. GPS, GLONASS, Galileo and more*. Springer, New York.

Kalita, J. (2017). *Analysis of factors that influence the quality of Precise Point Positioning method*. PhD Thesis. University of Warmia and Mazury in Olsztyn.

Kazmierski, K., Hadas, T. and Sośnica, K. (2018). Weighting of Multi-GNSS Observations in Real-Time Precise Point Positioning. *Remote Sens.*, 10(1), 84. DOI: 10.3390/rs10010084.

Khodabandeh, A. and Teunissen, P.J.G. (2015). An analytical study of PPP-RTK corrections: precision, correlation and user-impact. *Journal of Geodesy* 89(11), 1–24. DOI: 10.1007/s00190- 015-0838-9.

Kouba, J. and Heroux, P. (2001). GPS Precise Point Positioning Using IGS Orbit Products. *Solutions*, 5(2), 12–28.

Kouba, J. (2015). A guide to using international GNSS service (IGS) products, September 2015 update. http://kb.igs.org/hc/en-us/articles/201271873-A-Guide-to-Using-the-IGS-Products.

Kouba, J., Lahaye, F. and Tétreault, P. (2017). *Precise Point Positioning*. Springer Handbook of Global Navigation Satellite Systems. Springer Handbooks, Springer, Cham.

Kostelecky, J., Dousa, J., Kostelecky, J. (jr) and Vaclavovic, P. (2015). Analysis of the time series of station coordinates – a comparison of the network and PPP approach. *Acta Geodyn. Geomater.*, Vol. 12, No 2(178), 127–133. DOI: 10.13168/AGG.2015.0019.

Krzan, G. and Stępniak, K. (2017). Application of the undifferenced GNSS precise positioning in determining coordinates in national reference frames. *Artificial Satellites*, 52(3), 49–69.

Li, X., Ge, M., Lu, C., Zhang, Y., Wang, R., Wickert, J. and Schuh, H. (2014a). High-rate GPS seismology using real-time precise point positioning with ambiguity resolution. *IEEE Transactions on Geoscience and Remote Sensing*, 52(10), 6165–6180. DOI: 10.1109/TGRS.2013.2295373.

Li, X., Dick, G., Ge, M., Heise, S., Wickert, J. and Bender, M. (2014b). Real-time GPS sensing of atmospheric water vapor: Precise point positioning with orbit, clock, and phase delay corrections. *Geophys. Res. Lett.*, 41, 3615–3621. DOI: 10.1002/2013GL058721.

Li, X., Ge, M., Dai, X., Ren, X., Fritsche, M., Wickert, J. and Schuh, H. (2015). Accuracy and reliability of multiGNSS real-time precise positioning: GPS, GLONASS, BeiDou, and Galileo. *J. Geod.*, 89(6), 607–635.

Liu Z, Li, Y., Jinyun, G. and Li, Fei. (2016). Influence of higher-order ionospheric delay correction on GPS precise orbit determination and precise positioning. *Geodesy and Geodynamics*, 7, 369–376. DOI: 10.1016/j.geog.2016.06.005.

Liu, T., Yuan, Y., Zhang, B., Wang, N., Tan, B. and Chen, Y. (2017). Multi-GNSS precise point positioning (MGPPP) using raw observations. *J. Geod.*, 91, 253–268.

Lou, Y., Zhang, W., Wang, C., Yao, X., Shi, C. and Liu J. (2014). The impact of orbital errors on the estimation of satellite clock errors and PPP. *Adv Space Res*, 54(8), 1571–1580.

Nistor, S. and Buda, A.S. (2016). High rate 30 seconds vs clock interpolation in precise point positioning (PPP). *Geodetski vestnik*, 60(3), 483–494. DOI: 10.15292/geodetski-vestnik.2016.03.483-494.

Nykiel, G. and Figurski, M. (2016). Precise Point Positioning Method Based on Wide-lane and Narrow-lane Phase Observation and Between Satellites Single Differencing. *Proceedings of the 2016 International Technical Meeting*, ION ITM 2016, Monterey, California, January 25-28, 2016.

Paziewski, J. and Wielgosz, P. (2017). Investigation of some selected strategies for multi-GNSS instantaneous RTK positioning. *Advances in Space Research*, 59(1), 12–23. DOI: 10.1016/j.asr.2016.08.034.

Prochniewicz, D., Szpunar, R. and Walo, J. (2016). A new study of describing the reliability of GNSS Network RTK positioning with the use of quality indicators. *Meas. Sci. Technol*., 28.

Rabbou, M.A. and El-Rabbany, A. (2015). PPP accuracy enhancement using GPS/GLONASS observations in kinematic mode. *Positioning*, 6(1), 1–6. DOI: 10.4236/pos.2015.61001.

Rabbou, M.A. and El-Rabbany A. (2016). Performance analysis of precise point positioning using multi-constellation GNSS: GPS, GLONASS, Galileo and BeiDou. *Survey Review*. DOI: 10.1080/00396265.2015.1108068.

Rothacher, M., Springer, T. A., Schaer, S. and Beutler, G. (1998). *Processing strategies for regional GPS networks*. In: Brunner, F.K., editor, Advances in Positioning and Reference Frames, volume 118 of International Association of Geodesy Symposia, pages 93–100. Springer Berlin Heidelberg, 1998. DOI: 10.1007/978-3-662-03714-0_14.

RTCA-MOPS. (2006). Minimum Operational Performance Standards for Global Positioning System/ Wide Area Augmentation System Airborne Equipment.rtca document 229-C.

Sanz Subirana J., Juan Zornoza J.M. and Hernández-Pajares M. (2013). *GNSS Data Processing*, Vol. 1: *Fundamentals and Algorithms*, ESA TM-23/1, May 2013.

Shi, J., and Gao, Y. (2009). Assimilation of GPS Radio Occultation Observations with a Near Real-Time GPS PPP-Inferred Water Vapor System. *Proceedings of the 22nd International Technical Meeting of The Satellite Division of the Institute of Navigation* (ION GNSS 2009), Savannah, GA, September 2009, pp. 2584–2590.

Tegedor, J, Ovstedal, O. and Vigen, E. (2014). Precise orbit determination and point positioning using GPS, Glonass, Galileo and BeiDou. *Journal of Geodetic Science*, 4(1), 2081–9943, DOI: 10.2478/jogs-2014-0008.

Teunissen, P.J.D., Odijk, D. and Zhang, B. (2010). PPP-RTK: results of CORS network-based PPP with integer ambiguity resolution. *J. Aeronaut.*, 42(4), 223–229.

Tsai, M.L., Chiang, K.W., Lo, C.F. and Ch, C.H. (2013). The Performance Analysis of a Uav Based Mobile Mapping System Platform. *ISPRS – International Archives of the Photogrammetry, Remote Sensing and Spatial Information Sciences*, Volume XL-1/W2, 407–411.

Wang, L., Li, Z., Ge, M., Neitzel, F., Wang, Z. and Yuan, H. (2108). Validation and Assessment of Multi-GNSS Real-Time Precise Point Positioning in Simulated Kinematic Mode Using IGS Real-Time Service. *Remote Sens.*, 10, 337.

Witchayangkoon, B. (2002). *Elements of GPS Precise Point Positioning*. M.Sc.Thesis, the University of Maine December.

Yu, X. and Gao, J. (2017). Kinematic Precise Point Positioning Using Multi-Constellation Global Navigation Satellite System (GNSS) Observations. *ISPRS Int. J. Geo-Inf.*, 6, 6.

Zumberge, J.F., Helfin, M.B., Jefferson, D.C., Watkins, M.M. and Webb, F.H. (1997). Precise Point Processing for the Efficient and Robust Analysis of GPS Data from Large Networks. *Journal of Geophysical Research*, 102(B3), 5005–5017.